Asymmetric Behavior of Severed Microtubule Ends After Ultraviolet-Microbeam Irradiation of Individual Microtubules In Vitro

R. A. Walker, Shinya Inoué,* and E. D. Salmon

Department of Biology, University of North Carolina, Chapel Hill, North Carolina 27599-3280; and
*Marine Biological Laboratory, Woods Hole, Massachusetts 02543

Abstract. The molecular basis of microtubule dynamic instability is controversial, but is thought to be related to a "GTP cap." A key prediction of the GTP cap model is that the proposed labile GDP-tubulin core will rapidly dissociate if the GTP-tubulin cap is lost. We have tested this prediction by using a UV microbeam to cut the ends from elongating microtubules. Phosphocellulose-purified tubulin was assembled onto the plus and minus ends of sea urchin flagellar axoneme fragments at 21–22°C. The assembly dynamics of individual microtubules were recorded in real time using video microscopy. When the tip of an elongating plus end microtubule was cut off, the severed plus end microtubule always rapidly shortened back to the axoneme at the normal plus end rate. However, when the distal tip of an elongating minus end microtubule was cut off, no rapid shortening occurred. Instead, the severed minus end resumed elongation at the normal minus end rate. Our results show that some form of "stabilizing cap," possibly a GTP cap, governs the transition (catastrophe) from elongation to rapid shortening at the plus end. At the minus end, a simple GTP cap is not sufficient to explain the observed behavior unless UV induces immediate recapping of minus, but not plus, ends. Another possibility is that a second step, perhaps a structural transformation, is required in addition to GTP cap loss for rapid shortening to occur. This transformation would be favored at plus, but not minus ends, to account for the asymmetric behavior of the ends.

MICROTUBULES assembled from purified tubulin in vitro exhibit dynamic instability (21, 34, 45). After nucleation, individual microtubules alternate between an elongation phase and a rapid shortening phase (except those that shorten to completion). The transition (catastrophe) from elongation to rapid shortening and the transition (rescue) from rapid shortening to elongation are abrupt, stochastic, and infrequent in comparison to the rates of tubulin association and dissociation. Microtubules are polarized polymers and, in vitro, both the fast-growing plus ends and the slow-growing minus ends exhibit dynamic instability (21, 45). Several different experimental approaches have shown that the majority of plus end microtubules in vivo also exhibit dynamic instability (9–11, 37, 39, 41, 42).

A "GTP cap" model has been proposed to explain dynamic instability (19, 20, 34). It has been well established that GTP-tubulin adds to the end of an elongating microtubule, and that the bound GTP is subsequently hydrolyzed to GDP (4, 5, 7, 13, 30, 36). The GTP cap model postulates that this hydrolysis produces a labile "core" of GDP-tubulin subunits "capped" at the elongating end by newly added GTP-tubulin (the "GTP cap") (5, 6, 34). According to the model, catastrophe is the loss of the GTP cap, and rapid shortening follows due to the high rate of GDP-tubulin dissociation. Rescue is thought to occur when a rapidly shortening end becomes recapped with GTP-tubulin, a process which is infrequent in comparison to the rate of GDP-tubulin dissociation. Although the mechanism and location of GTP hydrolysis within a microtubule is controversial and unresolved (2, 4, 5, 7, 8, 12, 34, 36, 40, 45), there is substantial support for the GTP cap hypothesis: (*a*) the bulk of polymer is GDP-tubulin (17, 29, 30, 36, 46, 47); (*b*) elongation and rapid shortening are distinctly different phases (6, 21, 34, 45); (*c*) GDP-tubulin subunits do not support elongation in buffers which permit dynamic instability (3); (*d*) rapid shortening occurs within seconds at both ends when GTP-tubulin association is prevented by dilution (Voter, W. A, and H. P. Erickson, manuscript in preparation; Walker, R. A., and E. D. Salmon, unpublished observations); (*e*) addition of a GTPase system to microtubules at steady-state results in polymer disassembly (3); (*f*) for both ends, dissociation during the rapid shortening phase typically occurs at a constant rate as expected for a homogeneous core of GDP-tubulin subunits (21, 45); (*g*) for both ends, there is a substantial dissociation rate during the elongation phase without any apparent phase transition (45); and (*h*) the critical concentration for elongation is similar at the two ends, suggesting that there is reversible dissociation (of GTP-tubulin subunits) at both ends (45).

The GTP cap model makes a simple prediction about the behavior of severed microtubule ends (Fig. 1): cutting the elongating end from a microtubule will produce severed plus and minus ends with exposed GDP-tubulin subunits. If the

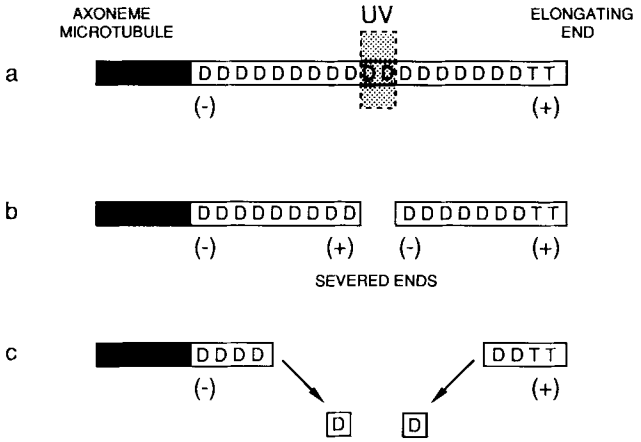

Figure 1. Predicted behavior of severed microtubule ends based on the GTP cap model. Schematic drawing of tubulin subunits in a microtubule growing from one end of an axoneme fragment (*solid area*). According to the GTP cap model (7, 19, 20, 34), the incorporation of GTP-tubulin (*T*) subunits at the elongating end of the microtubule stabilizes a labile core of GDP-tubulin (*D*) (the result of hydrolysis following subunit addition) (*a*). When the microtubule core is cut by UV irradiation (*b*), two severed ends are created, one plus, the other minus. The GTP cap model predicts that both severed ends will rapidly shorten (*c*) because they are no longer stabilized by GTP-tubulin.

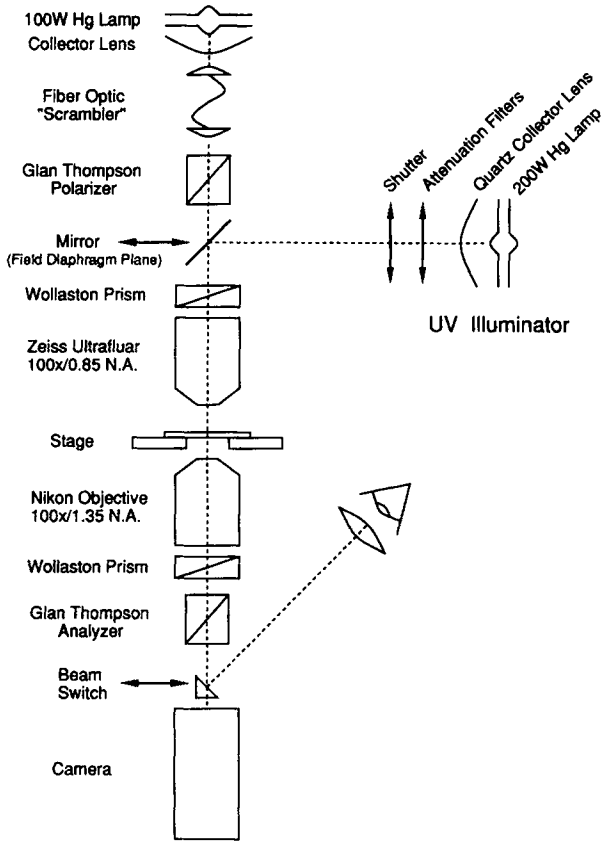

Figure 2. Schematic diagram of the UV microbeam apparatus. A 200-W mercury arc lamp served as the UV source. The microbeam was directed onto the specimen plane from the condenser side by a mirror inserted at the field diaphragm plane. A 100×/0.85 NA Zeiss Ultrafluar (Thornwood, NY) was used as the condenser. A 2-μm-wide image of the UV mirror was projected onto the specimen. The Wollaston DIC prism transmitted sufficient UV (~20%) to sever microtubules with a 3-s exposure. Shutters controlled the UV irradiation. Design details for the differential interference contrast optics, video recording, and digital image processing are described in the text.

GTP cap model is correct, these severed ends should begin rapid shortening immediately after cutting.

To test the GTP cap prediction illustrated in Fig. 1, we have used a UV microbeam to sever individual, elongating microtubules. A UV source and the necessary UV-transmitting optics were incorporated into a custom-designed light microscope (Fig. 2). Purified tubulin was assembled onto the plus and minus ends of sea urchin flagellar axoneme fragments using the methods of Walker et al. (45). The behavior of severed ends was observed and recorded in real time using video-enhanced differential interference contrast (DIC) microscopy and digital image processing. Contrary to the prediction of the GTP cap model, the plus and minus ends behave quite differently.

Materials and Methods

Tubulin and Axoneme Preparation

Porcine brain tubulin was purified by two cycles of assembly and disassembly in a buffer of 100 mM Pipes, 2 mM EGTA, 1 mM $MgSO_4$, 0.5 mM GTP, pH 6.9 (PM buffer) and the resulting pellets were overlaid with a buffer of 100 mM 2[*N*-morpholino]ethanesulfonic acid (MES), 1 mM EGTA, 0.5 mM $MgSO_4$, 3.4 M glycerol, pH 6.6. The tubulin was resuspended and passed over phosphocellulose and further purified by a cycle of assembly in 1 M Na^+-glutamate as described previously (44). The tubulin was then resuspended immediately in PM buffer and frozen in small aliquots. Based on the SDS-PAGE methods described in Walker et al. (45), microtubule-associated proteins constituted ~0.6% of the purified tubulin preparation. Flagellar axoneme fragments were prepared from *Lytechinus pictus* according to the method of Bell et al. (1). Axonemes were osmotically demembranated and mechanically separated from sperm heads by homogenization in a solution of 20% sucrose in distilled water with a hand-held glass homogenizer. Axonemes were resuspended and washed in isolation buffer composed of 0.1 mM NaCl, 4 mM $MgSO_4$, 1 mM EDTA, 7 mM β-mercaptoethanol, and 10 mM Hepes (pH 7.0). Dynein outer arms were removed by incubation in isolation buffer adjusted to 0.6 M NaCl for 30 min at 4°C. Residual sperm heads were removed by sedimentation of the axonemes through an 80% sucrose cushion (16,000 *g*, 10 min). Axonemes were stored at −20°C in a 1:1 solution of isolation buffer/glycerol. Axonemes were washed and resuspended in PM before use.

Microscopy and the UV Microbeam

Preparations were viewed by DIC microscopy, using a custom-built, inverted polarization microscope (22, 24, 25). The image of the UV source, an HBO 200-W mercury arc lamp, was projected onto a 0.2 × 0.7 mm mirror inserted in the field diaphragm plane of the microscope after the visible illuminating beam had passed the polarizing prism (Fig. 2). A Zeiss Ultrafluar 100×/0.85 NA glycerin immersion objective (Thornwood, NY) served as the condenser and was equipped with a Wollaston prism from a Zeiss 63×/1.4 NA objective lens. This combination provided a reasonable match to the Nomarski type prism made for Nikon Plan Apo objectives. The Ultrafluar projected a 2-μm-wide image of the illuminated mirror (the UV slit) onto the specimen plane, superimposed on the visible light DIC image of the specimen. The mirror could be slid in and out of the light path. With the mirror in the light path, the image of the UV source was first focused onto the specimen through UV blocking and neutral density filters. The filters were removed to expose the microtubule to the UV microbeam. A Nikon Plan Apo 100×/1.35 NA oil immersion objective projected the specimen image through a Nikon Nomarski DIC prism and analyzing prism to either the oculars or a video camera.

Image contrast was enhanced by video and digital processing. Video enhancement was provided by a newvicon video camera with high gain and offset (model 65, Dage-MTI Inc., Michigan City, IN), followed by digital enhancement provided by an Image-I/AT processor (Universal Imaging Corp., Media, PA). An exponential average of two frames with background mottle subtraction was used on-line to reduce electronic and optical noise in the image. Processed images were recorded on 3/4 inch U-matic tape (Sony model VO-5800H videocassette recorder) and optical disk (Panasonic model TQ-2021FBC optical memory disk recorder).

UV Irradiation Experiments

Purified tubulin and axonemes were mixed and then diluted with cold PM to final concentrations of 16 μM and 2.7 $\times$ 10^7 ml^{-1}, respectively. Preparations contained 1 mM GTP. The tubulin-axoneme preparation was held at 4°C until needed.

A 5-μl sample of the preparation was added to a biologically clean (32) 22-mm^2 quartz coverslip (thickness No. 1.5) mounted on a stainless steel holder, then covered with a biologically clean 22-mm^2 glass coverslip (thickness No. 1.5) and sealed with valap (1:1:1 mixture of beeswax, lanolin, and petrolatum) to prevent drying and to prevent flow within the chamber. The typical separation between inner chamber surfaces was 10–20 μm. The double coverslip chamber was inverted and glycerol and oil contacted to the Ultrafluar and Plan Apo lenses, respectively.

Microtubules were assembled at 21–22°C. The axoneme fragments adhered to the clean chamber surfaces but the microtubules elongating off of these fragments generally remained in solution. Microtubules that did adhere to the coverslip surface could not be severed by UV irradiation.

Microtubules were typically irradiated 15–40 min after initiation of assembly. Microtubules irradiated at longer times behaved identically (in terms of response to cutting) to microtubules irradiated soon after initiation of assembly.

Exposures of 2–3 s of unfiltered UV irradiation faithfully severed elongating microtubules. Based on previous studies (31, 48), irradiation in the 260–300 nm range severs microtubules in vivo.

Data Analysis

Microtubule elongation and plus end rapid shortening rates were measured from 3/4 inch U-matic videotape recordings played on a Sony VO-5800H. We used a computer-based analysis system to follow microtubule length changes in real time (45). Minus end shortening rates were difficult to measure in real time because of the brief duration of rapid shortening episodes. Minus end shortening rates were therefore calculated as (change in length)/(time of rapid shortening) for each episode.

Plus and minus ends were identified based on rate of elongation (45). Rates in the text are given as mean $\pm$ SEM.

Results

Experiments were performed at 21–22°C to prevent thermal damage to the microscope optics. At the tubulin concentration (16 μM) used in this study, a spontaneous catastrophe occurred at elongating plus ends about once every 4 min of elongation. Rescue was infrequent for plus end microtubules, and rapid shortening usually proceeded to the axoneme seed. At the minus end, a spontaneous catastrophe occurred about once every 15 min of elongation. Shortening

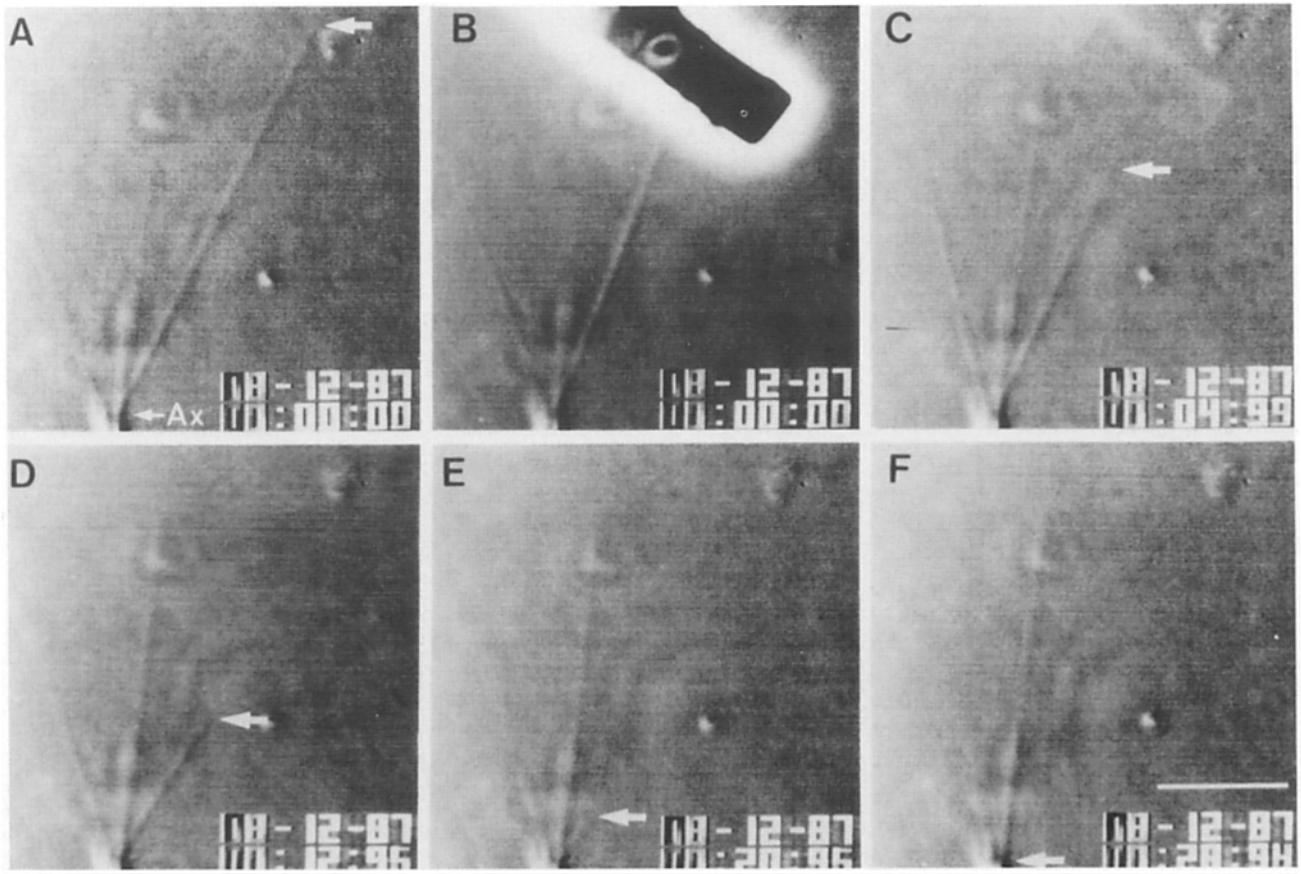

Figure 3. A severed plus end rapidly shortens immediately after UV cutting. The distal tip of an elongating plus end microtubule was cut off by 3 s UV irradiation. (*A*) Field before irradiation, Ax is plus end of axoneme fragment; (*B*) mirror in place just before UV irradiation; (*C*) 4 s after irradiation. An image of the irradiation beam persists on the camera tube. Arrowhead indicates the position of the severed plus end; (*D–F*) the severed plus end continues rapid shortening until it disappears. Time in minutes/seconds/0.01 seconds is given at the bottom right of each video frame. Bar, 5 μm.

minus end microtubules usually underwent rescue, and the average length lost during a shortening phase was 3.2 μm (based on average time of shortening and the mean rate of shortening).

Microtubule Irradiation

Each UV irradiation of an individual microtubule created two severed ends: one plus, the other minus. In practice, we were able to measure the resultant length changes of only the microtubules that remained tethered to the axoneme fragment. The other severed end, now one end of a free microtubule, was impossible to observe because the nascent free microtubule rapidly moved out of the plane of focus. Therefore, the behavior of severed plus end microtubules was observed by cutting microtubules which elongated off of the plus end of an axoneme fragment, whereas the behavior of severed minus end microtubules was observed by cutting microtubules which elongated off of an axoneme fragment's minus end.

All plus end microtubules severed by the UV microbeam immediately began rapid shortening (n = 16) (Figs. 3 and 5 *a*). The onset of rapid shortening was independent of the position of the cut zone relative to either the axoneme seed or the microtubule end. The minimum distance that we were able to remove from an elongating plus end microtubule was 0.8 μm. The rate of rapid shortening of a severed plus end microtubule (20.9 ± 1.5 μm/min [n = 15]) was not significantly different from the rapid shortening rate of a plus end microtubule that had experienced a spontaneous catastrophe (22.2 ± 1.7 μm/min [n = 8]) (independent t-test).

In contrast to the plus end, severed minus end microtubules never rapidly shortened (n = 29). Severed minus ends always remained within 0.2 μm (our limit of resolution) of the cut zone (Figs. 4 and 5, *b* and *c*) and then resumed elongation (Fig. 5, *b* and *c*). The stability of a severed minus end was independent of the amount of polymer removed from the elongating end as shown in Fig. 5 *b*. In this example, an elongating minus end microtubule was cut at successive times at distances progressively closer to the axoneme, but the severed minus ends never rapidly shortened.

The tubulin lattice at severed minus ends did not appear significantly altered because severed minus ends always immediately began elongation at rates (0.40 ± 0.03 μm/min [n = 28]) typical of normal minus end elongation (0.41 ± 0.04 μm/min [n = 14]) (independent t-test). Further, after reelongation, the region of a microtubule at the original cut site was no more stable than elsewhere along the microtubule. As shown in Fig. 5 *c*, severed minus end microtubules were observed to elongate until a spontaneous catastrophe occurred, then to rapidly shorten without interruption through the previous cut site. These observations demonstrate that UV irradiation did not prevent rapid shortening of minus ends by irreversibly cross-linking the microtubule lattice.

Discussion

According to the GTP cap model, a microtubule contains GDP-tubulin all along its length, except for a short region of GTP-tubulin at the elongating end(s) (Fig. 1). Cutting a microtubule at any site along its length (away from the GTP-tubulin cap) will produce severed ends with terminal GDP-tubulin subunits which will immediately dissociate. We have

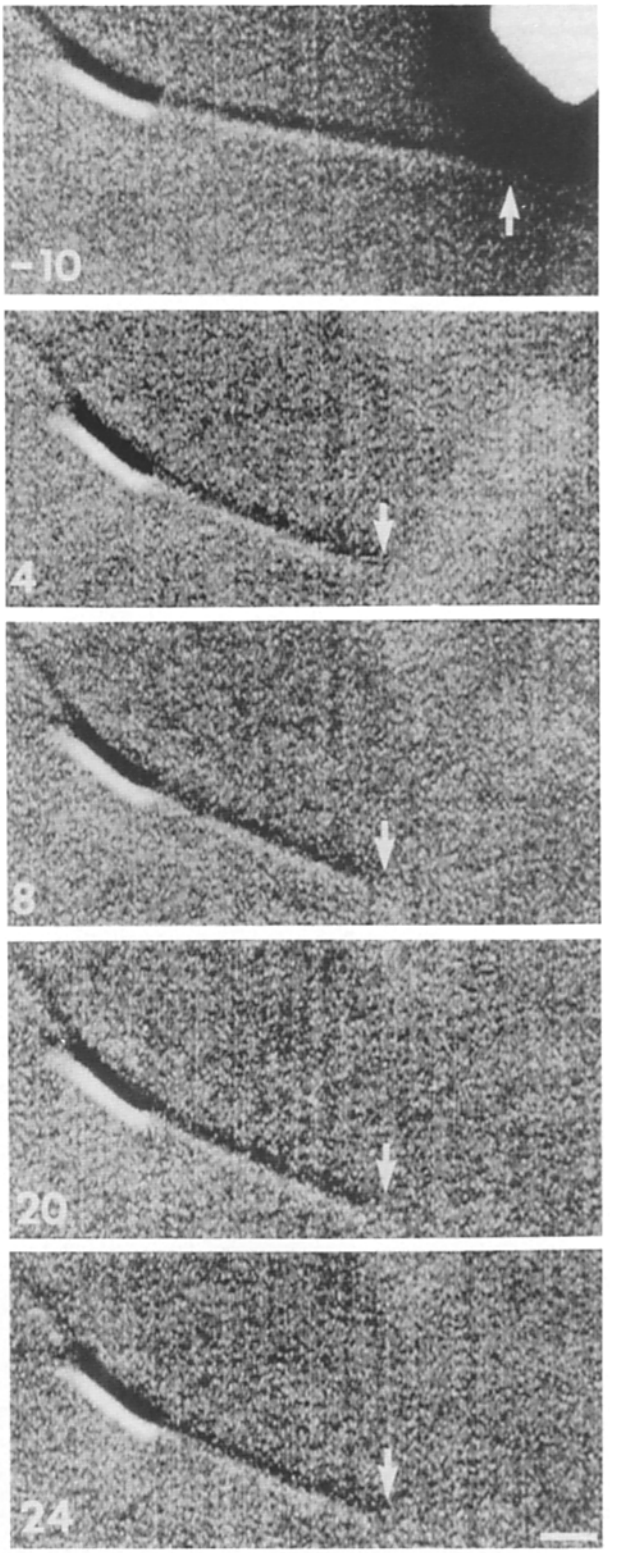

Figure 4. A severed minus end does not rapidly shorten after UV cutting. The distal tip of an elongating minus end microtubule was cut off by 3 s UV irradiation. Time is given in seconds on each video frame with the time of UV irradiation set to zero time. At 4 s, the image of the cutting zone (the UV irradiation area) persists on the video camera tube. The axoneme was slightly reoriented before exposure to the UV microbeam. The arrows indicate the microtubule end. Bar = 1 μm.

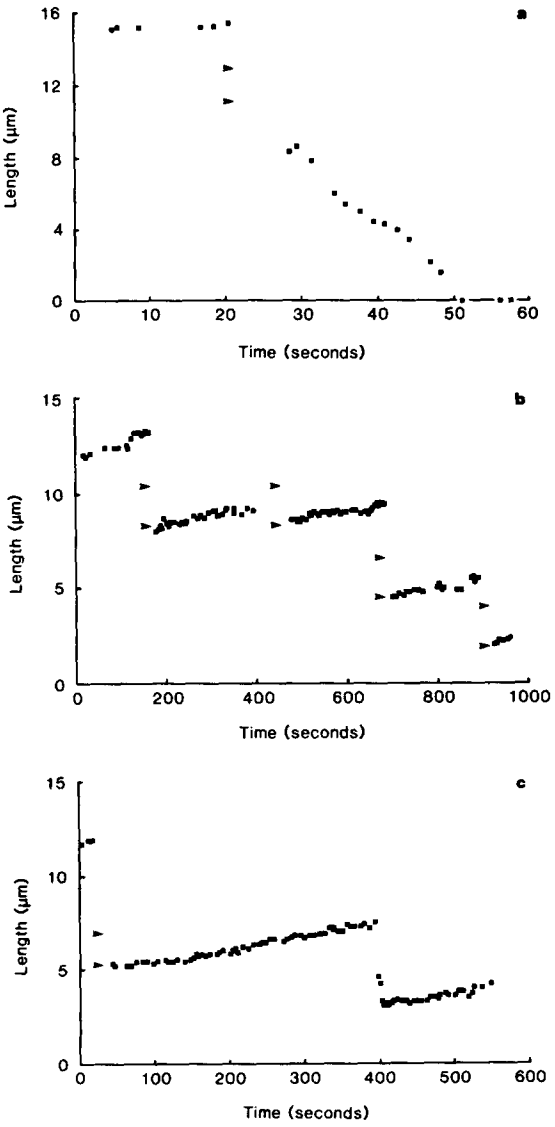

Figure 5. Behavior of severed plus and minus ends after UV cutting. Changes in microtubule length are plotted as a function of time. Length was measured from the end of the axoneme to the distal end of the attached microtubule. Arrowheads indicate width and location of the UV microbeam, and tips of the arrowheads indicate when the 3-s irradiation began. The portion of the microtubule distal to the cut zone always rapidly diffused out of view. (*a*) A plus end microtubule is irradiated and the severed end immediately starts to rapidly shorten. (*b*) A minus end microtubule was cut to successively shorter lengths but never rapidly shortened. (*c*) Microtubules experienced spontaneous catastrophes under the conditions used in this study. In this example, a severed minus end elongated for 2.3 μm, then underwent a spontaneous catastrophe and rapidly shortened for 4.4 μm. Note that the microtubule elongated from and shortened through the original cut site.

shown that severed plus end microtubules, as predicted by the GTP cap model, immediately begin to disassemble (summarized in Fig. 6, *a–c*). Rapid shortening was extensive and occurred at a constant rate both independent of the length of the microtubule and typical of spontaneous rapid shortening. Our results clearly demonstrate that a short region (<0.8 μm or 1,300 subunits) at the plus end of an elongating microtubule can stabilize the entire polymer.

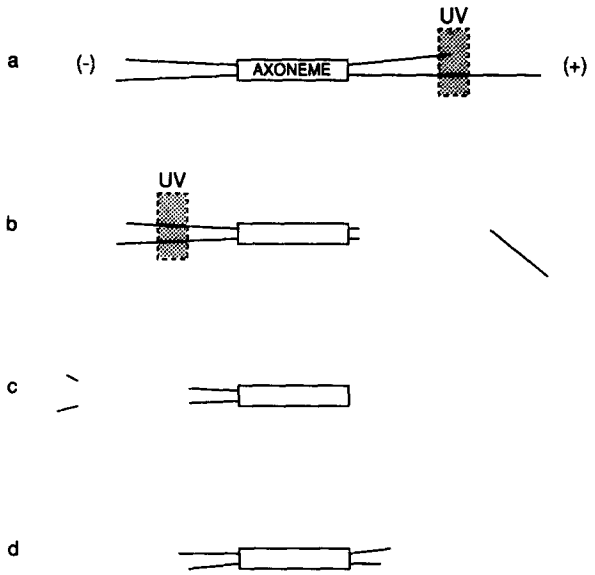

Figure 6. Summary of UV cutting experiments. Severed plus end microtubules (*a*), rapidly shortened (*b*), and frequently disappeared (*c*). Later, new plus end microtubules reelongated off of the axoneme fragment (*d*). In contrast, severed minus end microtubules (*b*), did not rapidly shorten, but immediately resumed elongation at a rate typical of minus end growth (*c* and *d*).

In contrast to the labile nature of severed plus ends, the stability of severed minus ends was not predicted by the GTP cap model. No shortening of severed minus end microtubules was detected; rather, these microtubules behaved as if capped by GTP-tubulin and immediately resumed elongation at rates typical of unsevered minus end microtubules (summarized in Fig. 6, *b–d*). Because the bulk of a microtubule is GDP-tubulin (17, 29, 30, 36, 46, 47), and because severed plus end microtubules initially appear to have terminal GDP-tubulin subunits (based on the behavior of severed plus ends), severed minus end microtubules must also initially have terminal GDP-tubulin subunits. How did severed minus end microtubules quickly regain a GTP cap? Our results show that UV irradiation did not irreversibly stabilize the microtubule lattice at the severed end. Further, the stability of severed minus ends was clearly not due to the "normal" mechanism of rescue (presumably addition of GTP-tubulin to GDP-tubulin ends), because the average extent of minus end rapid shortening after a spontaneous catastrophe was 3.2 μm, whereas the maximum extent of shortening for each severed minus end was 0.2 μm (our limit of resolution). Alternatively, the lattice structure of plus and minus end microtubules assembled onto an axoneme seed may be different. However, this does not seem likely because preliminary observations of UV severed microtubules self-assembled in the absence of axoneme seeds also show an asymmetric behavior: one end rapidly shortens while the other end is stable (Walker, R. A., and E. D. Salmon, manuscript in preparation).

There are two different explanations, based on the GTP cap model, for the difference in stability of severed plus and minus ends. The first assumes that formation of a severed end immediately produces a GDP-tubulin end capable of rapid shortening. That is, a severed end is initially an end in the rapid shortening phase. This is the basic prediction of the

current GTP cap models. If both plus and minus severed ends are initially in the rapid shortening phase, then the extremely rapid rescue of severed minus ends must be produced by a UV-activated mechanism not available at plus ends. According to this hypothesis, UV irradiation somehow promotes rapid reformation of a GTP-tubulin cap at minus, but not plus, severed ends. One possibility is that the exchangeable site for GTP on the tubulin dimer is exposed at the minus end but not the plus end. UV irradiation could rapidly displace the GDP from the exchangeable site, allowing free GTP to bind and stabilize the polymer before significant rapid shortening occurs. Because the exchangeable site is located on the β subunit of the tubulin dimer (18, 27, 35), this mechanism predicts that the β subunit is oriented towards the minus end of a microtubule and the α subunit is oriented towards the plus end. Unfortunately, the orientation of the tubulin dimer within the microtubule lattice is not yet known.

An alternative explanation is that loss of the GTP cap is not sufficient for rapid shortening. A second reaction may be required before GDP-tubulin subunits at the end of a microtubule can dissociate. Thus, there could be an intermediate phase between elongation and rapid shortening. According to this model, catastrophe is a two-step process. The first step, the transition from the elongation phase to the intermediate phase, depends on the presence or absence of a GTP cap. The second step, the transition from the intermediate phase to rapid shortening, may involve a structural transformation at the end of the polymer lattice (28) which, once initiated, produces rapid dissociation of GDP-tubulin subunits as the transformation propagates rearward along the microtubule lattice. Cutting an elongating microtubule can be viewed as creating severed ends in the intermediate phase. The behavior of a severed end will reflect the probabilities of transition from this intermediate phase to either elongation or rapid shortening. At the plus end, conversion from the intermediate phase to the rapid shortening phase is highly favored, since a severed plus end microtubule immediately begins rapid shortening. However, at the minus end, conversion from the intermediate phase to the elongation phase is favored, since a severed minus end microtubule immediately resumes elongation.

The dynamics of microtubule assembly has been studied in living cells using UV microbeam irradiation to sever microtubules (14, 16, 23, 31, 43, 48). It is worth reconsidering the results from these studies with respect to our in vitro findings. We have demonstrated here, for microtubules assembled from pure brain tubulin, that severed minus ends immediately start to elongate while severed plus ends rapidly shorten. A similar behavior can be seen in reports of the effect of UV microbeam irradiation on microtubules in the cytoplasmic microtubule complex in mammalian tissue culture cells (43), the central spindle microtubules of diatoms (31), the chromosomal fibers in the mitotic endosperm of *Haemanthus* (23), and the chromosomal fibers in the first meiotic spermatocytes of the grasshopper, *Trimeratropis maritima* (16). In all these examples, the minus ends of severed microtubules appeared stable while the plus ends rapidly shortened to various extents. The results of UV microbeam irradiation of chromosomal fibers in first meiotic spermatocytes by Forer and co-workers appears to be more complex (14, 48). Recent electron microscopy studies (48) of areas of reduced birefringence (ARBs) produced by UV irradiation of chromosomal fibers indicate that the poleward movement of ARBs may be the consequence of the difference in assembly dynamics of severed plus and minus ends rather than poleward flow of spindle fiber material as originally proposed (14) (later interpreted as treadmilling of tubulin subunits [26, 33]; see Forer [15] and Wilson and Forer [48] for discussion). However, this interesting question remains unresolved.

Overall, the above analysis indicates that because minus ends are relatively stable, microtubule dynamics in living cells is likely to be governed by the dynamics of their plus ends.

We thank Brenda Bourns for her careful preparation of the purified tubulin used in this study and for her assistance in the preparation of this paper. Vicki Petrie and Susan Whitfield assisted with figure preparation. Drs. Tim O'Brien, Bruce Telzer, and Leah Haimo provided many helpful comments. Finally, we are grateful to Lynne Cassimeris and Nancy Pryer for discussions about melted microtubule ends, and to Bob Knudson for assistance in the design and construction of the microbeam apparatus.

This work was supported by National Institutes of Health (NIH) grant GM 24364 and National Science Foundation (NSF) grant DCB-8616621 to E. D. Salmon and NIH grant R37 GN31617-06 and NSF grant DCB-8518672 to S. Inoué.

Received for publication 15 August 1988 and in revised form 2 November 1988.

References

1. Bell, C. W., C. Fraser, W. S. Sale, W.-J. Y. Tang, and I. R. Gibbons. 1982. Preparation and purification of dynein. *Methods Cell Biol.* 24: 373–397.
2. Caplow, M., and R. Reid. 1985. Directed elongation model for microtubule GTP hydrolysis. *Proc. Natl. Acad. Sci. USA.* 82:3267–3276.
3. Caplow, M., and J. Shanks. 1987. GTP requirement for in vitro and in vivo microtubule assembly and stability. *In* The Cytoskeleton in Cell Differentiation and Development. R. B. Maccioni and J. Arechaga, editors. IRL Press, Oxford, UK. 63–73.
4. Caplow, M., J. Shanks, and B. D. Brylawski. 1985. Concerning the location of the GTP hydrolysis site on microtubules. *Can. J. Biochem. Cell Biol.* 63:422–429.
5. Carlier, M.-F., and D. Pantaloni. 1981. Kinetic analysis of guanosine 5'-triphosphate hydrolysis associated with tubulin polymerization. *Biochemistry.* 20:1918–1924.
6. Carlier, M.-F., T. L. Hill, and Y.-D. Chen. 1984. Interference of GTP hydrolysis in the mechanism of microtubule assembly: an experimental study. *Proc. Natl. Acad. Sci. USA.* 81:771–775.
7. Carlier, M.-F., D. Didry, and D. Pantaloni. 1987. Microtubule elongation and guanosine 5'-triphosphate hydrolysis. Role of guanine nucleotides in microtubule dynamics. *Biochemistry.* 26:4428–4437.
8. Carlier, M.-F., D. Didry, R. Melki, M. Chabre, and D. Pantaloni. 1988. Stabilization of microtubules by inorganic phosphate and its structural analogues, the fluoride complexes of aluminum and beryllium. *Biochemistry.* 27:3555–3559.
9. Cassimeris, L. U., P. Wadsworth, and E. D. Salmon. 1986. Dynamics of microtubule depolymerization in monocytes. *J. Cell Biol.* 102:2023–2032.
10. Cassimeris, L. U., R. A. Walker, N. K. Pryer, and E. D. Salmon. 1987. Dynamic instability of microtubules. *Bioessays.* 7:149–154.
11. Cassimeris, L., N. K. Pryer, and E. D. Salmon. 1988. Real-time observations of microtubule dynamic instability in living cells. *J. Cell Biol.* 107:2223– 2231.
12. Chen, Y., and T. L. Hill. 1985. Monte Carlo study of the GTP cap in a five-start helix model of a microtubule. *Proc. Natl. Acad. Sci. USA.* 82: 1131–1135.
13. David-Pfeuty, T., H. P. Erickson, and D. Pantaloni. 1977. Guanosinetriphosphatase activity of tubulin associated with microtubule assembly. *Proc. Natl. Acad. Sci. USA.* 74:5372–5376.
14. Forer, A. 1965. Local reduction of spindle fiber birefringence in living *Nephrotoma surturalis* (Leow) spermatocytes induced by ultraviolet microbeam irradiation. *J. Cell Biol.* 25:95–117.
15. Forer, A. 1985. Does actin produce the force that moves a chromosome to the pole during anaphase? *Can. J. Biochem. Cell Biol.* 63:585–598.
16. Gordon, G. G. 1980. The control of mitotic motility as influenced by ultraviolet microbeam irradiation of kinetochore fibers. Ph.D. dissertation. University of Pennsylvania.

17. Hamel, E., J. K. Batra, A. B. Huang, and C. M. Lin. 1986. Effects of pH on tubulin-nucleotide interactions. *Arch. Biochem. Biophys.* 245:316–330.
18. Hesse, J., H. Maruta, and G. Isenberg. 1985. Monoclonal antibodies localize the exchangeable GTP-binding site in β- and not α-tubulins. *FEBS (Fed. Eur. Biochem. Soc.) Lett.* 179:91–95.
19. Hill, T. L. 1984. Introductory analysis of the GTP-cap phase-change kinetics at the end of a microtubule. *Proc. Natl. Acad. Sci. USA.* 81:6728–6732.
20. Hill, T. L., and Y.-D. Chen. 1984. Phase changes at the end of a microtubule with a GTP cap. *Proc. Natl. Acad. Sci. USA.* 81:5772–5776.
21. Horio, T., and H. Hotani. 1986. Visualization of the dynamic instability of individual microtubules by dark-field microscopy. *Nature (Lond.).* 321:605–607.
22. Inoué, S. 1961. Polarizing microscope: design for maximum sensitivity. *In* Encyclopedia of Microscopy. G. L. Clarke, editor. Reinhold Publishing Corp., New York. 480–485.
23. Inoué, S. 1964. Organization and function of the mitotic spindle. *In* Primitive Motile Systems in Cell Biology. R. Allen and N. Kamiya, editors. Academic Press, New York, 549–598.
24. Inoué, S. 1981. Video image processing greatly enhances contrast, quality, and speed in polarization-based microscopy. *J. Cell Biol.* 89:346–356.
25. Inoué, S. 1986. Video Microscopy. Plenum Publishing Corp., New York. 495.
26. Inoué, S., and H. Ritter. 1975. Dynamics of mitotic spindle organization and function. *In* Molecules and Cell Movement. S. Inoué and R. Stephens, editors. Raven Press, New York. 3–29.
27. Kirchner, K., and E.-M. Mandelkow. 1985. Tubulin domains responsible for assembly of dimers and protofilaments. *EMBO (Eur. Mol. Biol. Organ.) J.* 4:2397–2402.
28. Kirschner, M. W., and T. Mitchison. 1986. Microtubule dynamics. *Nature (Lond.).* 324:621.
29. Kobayashi, T. 1974. Nucleotides bound to brain tubulin and reconstituted microtubules. *J. Biochem. (Tokyo).* 76:201–204.
30. Kobayashi, T. 1975. Dephosphorylation of tubulin-bound guanosine triphosphate during microtubule assembly. *J. Biochem. (Tokyo).* 77:1193–1197.
31. Leslie, R. J., and J. D. Pickett-Heaps. 1984. Spindle microtubule dynamics following ultraviolet-microbeam irradiations of mitotic diatoms. *Cell.* 36:717–727.
32. Lutz, D. A., and S. Inoué. 1986. Techniques for observing living gametes and embryos. *Methods Cell Biol.* 27:89–110.
33. Margolis, R. L., L. Wilson, and B. I. Kiefer. 1978. Mitotic mechanism based on intrinsic microtubule behavior. *Nature (Lond.).* 272:450–452.
34. Mitchison, T., and M. Kirschner. 1984. Dynamic instability of microtubule growth. *Nature (Lond.).* 232:237–242.
35. Nath, J. P., G. F. Eagle, and R. H. Himes. 1985. Direct photoaffinity labeling of tubulin and guanosine 5'-triphosphate. *Biochemistry.* 24:1555–1560.
36. O'Brien, E. T., W. A. Voter, and H. P. Erickson. 1987. GTP hydrolysis during microtubule assembly. *Biochemistry.* 26:4148–4156.
37. Salmon, E. D., and P. Wadsworth. 1986. Fluorescence studies of tubulin and microtubule dynamics in living cells. *In* Applications of Fluorescence in the Biomedical Sciences. D. L. Taylor, A. S. Waggoner, R. F. Murphy, F. Lanni, R. R. Birge, editors. Alan R. Liss, Inc., New York. 377–403.
38. Sammak, P. J., and G. G. Borisy. 1988. Direct observation of microtubule dynamics in living cells. *Nature (Lond.).* 332:724–726.
39. Sammak, P. J., G. J. Gorbsky, and G. G. Borisy. 1987. Microtubule dynamics in vivo: a test of mechanisms of turnover. *J. Cell Biol.* 104:395–405.
40. Schilstra, M. J., S. R. Martín, and P. M. Bayley. 1987. On the relationship between nucleotide hydrolysis and microtubule assembly: studies with a GTP-regenerating system. *Biochem. Biophys. Res. Commun.* 147:588–595.
41. Schulze, E., and M. Kirschner. 1986. Microtubule dynamics in interphase cells. *J. Cell Biol.* 102:1020–1031.
42. Schulze, E., and M. Kirschner. 1988. New features of microtubule behavior observed in vivo. *Nature (Lond.).* 334:356–359.
43. Tao, W., R. J. Walter, and M. W. Berns. 1987. Laser-transected microtubules exhibit individuality of regrowth, however most free new ends of the microtubules are stable. *J. Cell Biol.* 107:1025–1035.
44. Voter, W. A., and H. P. Erickson. 1984. The kinetics of microtubule assembly. *J. Biol. Chem.* 259:10430–10438.
45. Walker, R. A., E. T. O'Brien, N. K. Pryer, M. Soboeiro, W. A. Voter, H. P. Erickson, and E. D. Salmon. 1988. Dynamic instability of individual microtubules analyzed by video light microscopy: rate constants and transition frequencies. *J. Cell Biol.* 107:1437–1448.
46. Weisenberg, R. C., G. G. Borisy, and E. W. Taylor. 1968. The colchicine-binding protein of mammalian brain and its relation to microtubules. *Biochemistry.* 7:4466–4479.
47. Weisenberg, R. C., W. J. Deery, and P. J. Dickinson. 1976. Tubulin nucleotide interactions during the polymerization and depolymerization of microtubules. *Biochemistry.* 15:4248–4254.
48. Wilson, P. J., and A. Forer. 1988. Ultraviolet microbeam irradiation of chromosomal spindle fibers produces an area of reduced birefringence and shears the microtubules, allowing study of the dynamic behavior of new free ends in vivo. *J. Cell Sci.* 91:455–468.